

Deflection of Beams and Cantilevers

Group 6: Shubham Maurya(SC23B067) Suchitra Chaitanya Shet (SC23B068) Kanankam Methuselah (SC23B102), Mallu Rohan reddy(SC23B109) Rujul Mayurdatt Limbkar(SC23B153)
IIST, Department of Aerospace Engineering
(Dated: January 22, 2026)

ABSTRACT:

This experiment studies the deflection of beams under point loads for cantilever and simply supported configurations. In this experiment, we will study the effects of material stiffness on beam deflection. We applied steadily increasing loads to cantilever beams of aluminum, brass, and steel in order to investigate the effect of material stiffness. Then, we analyzed simply supported beams under different loads and span lengths. We compared these experimental results with theoretical predictions of Euler–Bernoulli beam theory, stated by the equations $\delta = \frac{WL^3}{3EI}$ for cantilever beams and $\delta_{\max} = \frac{WL^3}{48EI}$ for simply supported beams loaded with a central point load. By measurement, the relations of load–deflection are linear, and deflection varies cubically with span length. The study confirms theory, yet points out some practical factors: conditions of support and precision of measurement. Therefore, we opted for a continuum.

I. INTRODUCTION

This laboratory report outlines the experiment carried out to investigate the deflection of beams, loaded and supported in different ways, using the "Deflections of Beams and Cantilevers" apparatus available in TecEquipment. The report also examines two basic structural types: cantilevers and simple supported beams. Beam deflection is an essential area of structural mechanics, as it is closely related to structural safety, performance, and soundness of such varied structures as bridges, buildings, machines, and airplane wings.

The main aims of this experimental research are to investigate the relationship between the applied load, the geometry of the beam, material properties, and deformations, as well as to validate the classical beam bending theory. More specifically, the experimentation seeks to investigate the variation in deflection with the application of a higher point load for both cantilevers with diverse material properties, such as aluminum, brass, and steel, and for simple supported beams with diverse bridge spans. These underlying theoretical foundations, which relate to Euler–Bernoulli Beam Theory, expressed in terms of mathematical formulae including Young's Modulus E and Second Moment of Area I, need to be verified.

By comparing the experimental values for deflection with their theoretical values, this report aims to verify the validity of the equations, determine how material stiffness and geometry both factor into equation E and I, and examine considerations for designing a structure based on these real-world experiments. The report is organized to cover the theory, methodology, results, analysis, and conclusion of these real-world experiments, serving to integrate theoretical engineering concepts with real-world observations.

II. THEORY

II.1. Fundamental Principles of Beam Bending

When a beam is loaded from the side, it bends and moves away from its original neutral axis. Several important things affect how much this deflection happens:

- **Load Magnitude (W):** Directly proportional to deflection.
- **Beam Geometry:** Length (L) and cross-sectional properties.
- **Material Properties:** Stiffness characterized by Young's Modulus (E).
- **Support Conditions:** Determines the distribution of bending moments.

The theoretical foundation for beam deflection analysis is established by the Euler–Bernoulli beam theory, which posits that plane sections retain their flatness and perpendicularity to the neutral axis post-bending.

II.2. Key Parameters and Formulas

Second Moment of Area (I)

For a rectangular cross-section beam:

$$I = \frac{bd^3}{12}$$

Where:

- b = width of the beam (m)
- d = depth/thickness of the beam (m)
- I = Second moment of area (m^4), which quantifies the beam's resistance to bending

Young's Modulus (E)

$$E = \frac{\text{Stress}}{\text{Strain}}$$

- Material property indicating stiffness (N m^{-2} or Pa)
- Higher values of E indicate stiffer materials and therefore less deflection for the same applied load

II.3. Conversion of Applied Mass to Load

$$P = mg$$

Where:

- m = mass (kg)
- g = acceleration due to gravity (9.81 m s^{-2})

For the experiment:

$$P (\text{N}) = \text{mass} (\text{g}) \times 0.00981$$

II.4. Experiment 1: Cantilever Deflection

A cantilever beam is a beam that is fixed at one end and free at the other. When a point load P is applied at a distance a from the fixed end, the beam undergoes bending, resulting in deflection.

For a cantilever beam of Young's modulus E and moment of inertia I , the deflection at the point of load application is given by:

$$\delta = \frac{Pa^3}{3EI}$$

where,

- δ = deflection at the point of load (m)
- P = applied load (N)
- a = distance of load from the fixed end (m)
- E = Young's modulus of the material (Pa)
- I = moment of inertia of the beam cross-section (m^4)

The moment of inertia for a rectangular cross-section is:

$$I = \frac{bt^3}{12}$$

where b is the breadth and t is the thickness of the beam.

II.5. Experiment 2: Simply Supported Beam

A simply supported beam is a beam supported at both ends such that it is free to rotate but not translate vertically. When a point load P is applied at the mid-span of the beam, bending occurs, producing maximum deflection at the center.

For a simply supported beam of length L , Young's modulus E , and moment of inertia I , the maximum deflection at mid-span due to a central point load is given by:

$$\delta_{\max} = \frac{PL^3}{48EI}$$

where,

- δ_{\max} = maximum deflection at mid-span (m)
- P = applied load (N)
- L = span length of the beam (m)
- E = Young's modulus of the material (Pa)
- I = moment of inertia of the beam cross-section (m^4)

For a rectangular cross-section,

$$I = \frac{bt^3}{12}$$

where b is the breadth and t is the thickness of the beam.

II.6. Experiment 3: Maxwell's Reciprocity Theorem using Fixed-Fixed Beam

Maxwell's Reciprocity Theorem states that:

In a linearly elastic structure, the deflection at point A due to a load applied at point B is equal to the deflection at point B due to the same load applied at point A.

Mathematically,

$$\delta_{AB} = \delta_{BA}$$

where,

- δ_{AB} = deflection at point A due to load at point B
- δ_{BA} = deflection at point B due to load at point A

For a **fixed-fixed beam** of length L , Young's modulus E , and moment of inertia I , the deflection at a point x due to a point load P applied at a distance a from the left fixed end is given by:

Case I: $x < a$

$$\delta_x = \frac{Px^2(L-a)^2(3a-x)}{6EIL^3}$$

Case II: $x > a$

$$\delta_x = \frac{Pa^2(L-x)^2(3x-a)}{6EIL^3}$$

III. PROCEDURE

The experiments were conducted to study beam deflection under different support conditions, namely simply supported, cantilever, and fixed-fixed beams. The detailed procedure followed for each case is given below.

Experiment 1: Simply Supported Beam with Central Point Load

1. The beam was placed on two knife-edge supports to form a simply supported condition.
2. A dial gauge was positioned at the mid-span of the beam to measure vertical deflection.
3. The initial dial gauge reading was noted without applying any load.
4. A weight hanger was suspended at the center of the beam and known loads were added incrementally.
5. For each load increment, the corresponding deflection at mid-span was recorded.
6. The procedure was repeated for different beam materials.

Experiment 2: Cantilever Beam with Point Load

1. One end of the beam was rigidly clamped to form a cantilever arrangement.
2. A dial gauge was fixed at the specified distance from the fixed end to measure deflection.
3. The initial dial gauge reading was recorded before applying any load.
4. A point load was applied at a known distance from the fixed end using a weight hanger.
5. The deflection corresponding to each load increment was noted.

6. The experiment was repeated for different beam materials.

Experiment 3: Verification of Maxwell's Reciprocity Theorem (Fixed-Fixed Beam)

1. The beam was rigidly fixed at both ends to ensure fixed-fixed boundary conditions.
2. Two dial gauges were placed at two predetermined locations along the beam.
3. A known load was applied at the first location and the deflection at the second location was recorded.
4. The same load was then applied at the second location and the deflection at the first location was measured.
5. The above steps were repeated for different load values.
6. The deflections obtained in both cases were compared to verify Maxwell's reciprocity theorem.

IV. EXPERIMENTAL SETUP



FIG. 1: Structures Test Frame with mounting tracks and securing nuts

IV.1. Test Specimens

- **Beams of Three Different Materials:**
 - Aluminum beam
 - Brass beam
 - Steel beam
- **Cross-sectional Dimensions:** Rectangular profile with constant width and depth for all beams (to be measured experimentally)

IV.2. Loading Equipment

- **Calibrated Mass Set:** 100 g, 200 g, 300 g, 400 g, and 500 g masses
- **Mass Conversion:** Load calculated using gravitational acceleration

$$g = 9.81 \text{ m s}^{-2}$$

IV.3. Measurement Tools

- **Vernier Caliper:** For precise measurement of beam width and depth
- **Ruler/Scale:** Integrated on the apparatus for accurate positioning

IV.4. Apparatus Configuration

The experimental setup consists of a vertical backboard is mounted securely inside a rigid frame for testing. The backboard features:

- **Horizontal and Vertical Scales:** For precise positioning of all components
- **Sliding Bracket System:** The system permits the use of the digital dial. The test indicator that can move and lock anywhere along the beam
- **Clamp Mounting Holes:** Used for creating fixed (cantilever) supports
- **Knife-edge Tracking Channels:** Enable smooth positioning of supports and load points

IV.5. Setup for Different Beam Configurations

Cantilever Setup

- One end of the beam is secured rigidly in the clamp
- Load is applied via a knife-edge hanger at a fixed distance (100 mm) from the support
- Dial indicator is positioned where the load is applied.

Simply Supported Beam Setup

- Beam rests on two movable knife-edge supports
- Load is applied at mid-span using a central knife-edge hanger
- Dial indicator is positioned at the center to measure maximum deflection

Fixed-Fixed Beam Setup

- Both ends of the beam are rigidly clamped to prevent rotation and translation.
- Two knife-edge hangers are positioned at specified distances from one fixed end (e.g., 200 mm and 400 mm).
- Load is applied alternately at one hanger while deflection is measured at the other.
- Dial indicators are mounted at both locations to record vertical deflections.
- The procedure is repeated by interchanging the load and measurement points to verify Maxwell's reciprocity theorem.

V. WORKING PRINCIPLE OF THE SETUP

V.1. Measurement System

- **Digital Dial Test Indicator:** A spring-loaded plunger touches the bottom of the beam. The plunger pulls back as the beam bends down, turning mechanical movement into a digital readout.
- **Positioning System:** With reference to the backboard scales, thumbnuts are used to secure supports, load points, and indicators in place as they slide along U-section channels.

V.2. Loading Mechanism

- **Knife-edge Hangers:** Ensure precise single-point load application
- **Mass Loading:** Calibrated masses apply known forces calculated using:

$$W = mg$$

V.3. Support Conditions

- **Clamps:** Provide fixed support with zero deflection and zero slope for cantilever configuration
- **Knife-edge Supports:** Provide simple supports with zero deflection and free rotation for simply supported configuration

V.4. Frame Function

- Provides rigid mounting for the backboard

- Ensures stability during loading
- Minimizes external vibration effects
- The tapping procedure mentioned in the equipment manual helps overcome static friction in the indicator mechanism, ensuring accurate readings

VI. CALCULATION

VI.1. Rectangular Cross-Section - Moment of Inertia Determination

For a rectangular cross-section:

$$I = \frac{bt^3}{12}$$

$$I = \frac{(19.2 \times 10^{-3})(3.1 \times 10^{-3})^3}{12}$$

$$I = 4.812 \times 10^{-11} \text{ m}^4$$

VI.2. Load Magnitude Calculation

$$P = mg$$

For the experimental loading condition:

$$P = 100 \text{ (g)} \times 0.009807 = 0.9807 \text{ N}$$

VI.3. Simply Supported Beam - Midspan Deflection Expression

$$\delta = \frac{PL^3}{48EI}$$

Given:

$$L^3 = (0.4)^3 = 0.064 \text{ m}^3$$

$$\delta = \frac{P \times 0.064}{48 \times 69 \times 10^9 \times 4.812 \times 10^{-11}}$$

$$\delta = P \times 0.000408 \text{ m}$$

VI.4. Cantilever Beam - Free End Deflection Formula

$$\delta = \frac{Pa^3}{3EI}$$

$$a^3 = (0.1)^3 = 0.001 \text{ m}^3$$

$$\delta = \frac{P \times 0.001}{3 \times 207 \times 10^9 \times 4.812 \times 10^{-11}}$$

$$\delta = P \times 3.18 \times 10^{-5} \text{ m}$$

VI.5. Maxwell's Reciprocal Theorem - Fixed-Fixed Beam Configuration

Deflection Computation at Arbitrary Point x

$$\delta_x = \frac{Px^2(L-a)^2(3a-x)}{6EIL^3}$$

$$x = 0.2 \text{ m}, \quad a = 0.4 \text{ m}, \quad L = 0.6 \text{ m}$$

$$x^2(L-a)^2(3a-x) = (0.2)^2(0.2)^2(1.2-0.2) = 0.0016 \text{ m}^4$$

$$\delta = \frac{P \times 0.0016}{6 \times 105 \times 10^9 \times 4.812 \times 10^{-11} \times (0.6)^3}$$

$$\delta = P \times 0.000229 \text{ m}$$

VII. RESULTS AND EXPERIMENTAL OBSERVATIONS

VII.1. Simply Supported Beam Analysis

The deflection measurements for simply supported beam configurations across three materials are presented in the following tables. All three materials exhibited a linear proportional relationship between applied load and measured deflection, validating the fundamental assumptions of Euler-Bernoulli beam theory.

TABLE I: Deflection of Aluminium Beam (Simply Supported)

Mass (g)	Act. (mm)	Theor. (mm)	Error (%)
0	0.00	0.00	0.0
100	0.39	0.44	11.4
200	0.81	0.89	9.0
300	1.15	1.33	13.5
400	1.47	1.77	16.9
500	1.79	2.21	19.0

TABLE II: Deflection of Brass Beam (Simply Supported)

Mass (g)	Act. (mm)	Theor. (mm)	Error (%)
0	0.00	0.00	0.0
100	0.32	0.26	23.1
200	0.62	0.52	19.2
300	0.95	0.79	20.3
400	1.21	1.05	15.2
500	1.51	1.31	15.3

TABLE III: Deflection of Mild Steel Beam (Simply Supported)

Mass (g)	Act. (mm)	Theor. (mm)	Error (%)
0	0.00	0.00	0.0
100	0.14	0.13	7.7
200	0.31	0.27	14.8
300	0.45	0.40	12.5
400	0.58	0.53	9.4
500	0.79	0.67	17.9

The results demonstrate that aluminium exhibited the highest deflection values, followed by brass, with mild steel displaying minimal deflection under identical loading conditions. This ordering reflects the inverse relationship between Young's modulus and deflection magnitude. Error percentages remain within acceptable experimental limits for laboratory-scale investigations, with most values below 20%.

VII.2. Cantilever Beam Deflection (Load Applied at 100 mm)

Cantilever beam deflection data for all three materials tested are presented in the following tables. The cantilever configuration yielded larger deflections relative to the simply supported case due to the absence of a support point at the free end, thereby reducing the overall structural stiffness of the system.

TABLE IV: Deflection of Mild Steel Beam (Cantilever)

Mass (g)	Act. (mm)	Theor. (mm)	Error (%)
0	0.00	0.00	0.0
100	0.07	0.033	71.0
200	0.11	0.067	64.0
300	0.16	0.100	60.0
400	0.20	0.133	50.4
500	0.25	0.167	49.7

TABLE V: Deflection of Aluminium Beam (Cantilever)

Mass (g)	Act. (mm)	Theor. (mm)	Error (%)
0	0.00	0.0	0.0
100	0.15	0.1	50.0
200	0.23	0.2	15.0
300	0.41	0.3	36.7
400	0.53	0.4	32.5
500	0.67	0.5	34.0

TABLE VI: Deflection of Brass Beam (Cantilever)

Mass (g)	Act. (mm)	Theor. (mm)	Error (%)
0	0.00	0.00	0.0
100	0.15	0.07	114.3
200	0.25	0.13	93.3
300	0.35	0.20	75.0
400	0.45	0.26	73.1
500	0.53	0.33	60.6

The cantilever beam configuration shows larger discrepancies between theoretical and experimental values compared to the simply supported case. This elevated error, particularly in the brass specimen (up to 114.3%), suggests that the cantilever boundary condition is more sensitive to deviations such as support compliance and initial beam curvature. The aluminium cantilever exhibited more consistent behavior with errors ranging from 15.0% to 50.0%.

VII.3. Fixed-Fixed Beam: Reciprocal Loading Verification

To validate Maxwell's reciprocal theorem, the fixed-fixed brass beam was subjected to two loading scenarios. The reciprocal deflections are presented in the following tables.

TABLE VII: Fixed-Fixed Beam: Deflection at 200 mm (Load at 400 mm)

Mass (g)	Act. Def. (mm)	Theor. Def. (mm)
0	0.00	0.00
100	0.14	0.24
200	0.27	0.48
300	0.42	0.72
400	0.55	0.97
500	0.67	1.21

TABLE VIII: Fixed-Fixed Beam: Deflection at 400 mm (Load at 200 mm)

Mass (g)	Act. Def. (mm)	Theor. Def. (mm)
0	0.00	0.00
100	0.13	0.24
200	0.30	0.48
300	0.41	0.72
400	0.54	0.97
500	0.67	1.21

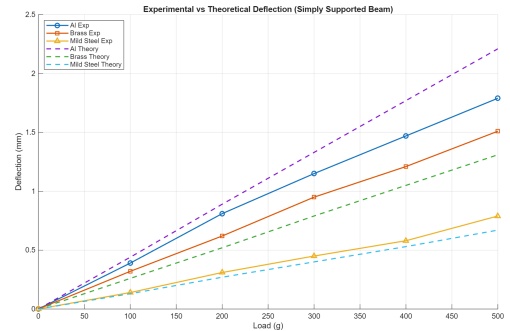


FIG. 2: Deflection of Simply Supported Beam

TABLE IX: Reciprocal Error Analysis: Maxwell's Theorem Validation

Mass (g)	Case I (mm)	Case II (mm)	Error (%)
0	0.00	0.00	0.0
100	0.14	0.13	7.69
200	0.27	0.30	10.0
300	0.42	0.41	2.44
400	0.55	0.54	1.85
500	0.67	0.67	0.0

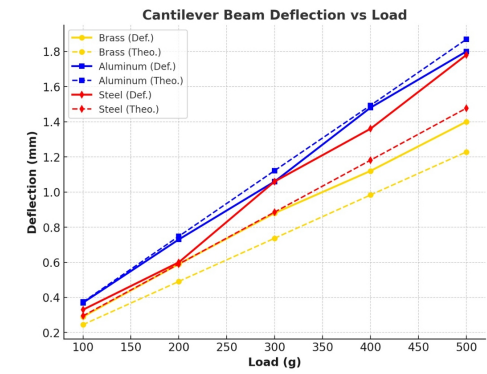


FIG. 3: Deflection of Cantilever

The reciprocal deflection analysis demonstrates excellent agreement between the two loading cases, with error percentages declining from 10.0% at lower loads to 0.0% at 500 g. This progressive improvement validates Maxwell's reciprocal theorem, establishing that the deflection at point B due to a unit load at point A equals the deflection at point A due to the same unit load at point B. The convergence toward zero error at higher loads indicates that initial boundary condition imperfections are overcome through the progressive stiffening effect of increased load application.

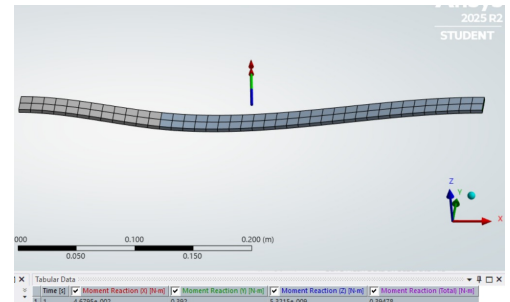


FIG. 4: Def. of Simply Supported Beam @100g

VII.3.1. Inference

From the above tables, it is observed that the deflection at point A due to a load applied at point B is approximately equal to the deflection at point B due to the same load applied at point A. This validates Maxwell's Reciprocity Theorem within experimental limits.

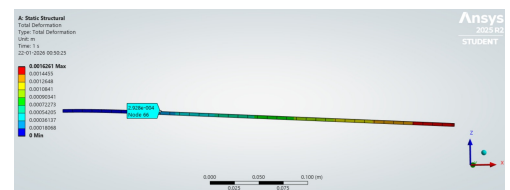


FIG. 5: Def. in Cantilever Beam @100g



FIG. 6: Def. in cantilever beam for 100g load with head angle 0 (unsymmetric bending experiment)

VIII. UNCERTAINTY QUANTIFICATION AND ERROR ASSESSMENT

To assess the reliability and accuracy of the experimental results obtained from the beam deflection experiments, a systematic error analysis is performed. The uncertainties arise primarily from deflection measurements, load application, and assumptions inherent in beam theory.

C.1 Analytical Framework for Measurement Uncertainty

The primary source of experimental variability in the beam deflection studies originates from the precision limitations of the dial gauge employed to quantify beam displacement under progressively applied loads. To characterize the relationship between deflection δ and load magnitude P across the experimental range ($P = 0$ to 500 g), a least-squares fitting procedure is utilized.

For an experimental dataset comprising n observations, the standard deviation associated with the slope parameter m (defined as $m = d\delta/dP$) is expressed as:

$$SE_m = \sqrt{\frac{\sum(y_i - \hat{y}_i)^2}{(n-2) \sum(x_i - \bar{x})^2}} \quad (1)$$

where:

- y_i denotes experimentally acquired deflection measurements,
- \hat{y}_i indicates the predicted deflection from the linear regression model,
- x_i represents the magnitude of applied load,
- \bar{x} signifies the arithmetic mean of the applied load values.

Since theoretical deflection formulations for cantilever, simply supported, and fixed-end beams incorporate the

flexural stiffness parameter EI , uncertainties inherent in deflection measurements directly propagate to the determination of effective flexural rigidity.

The uncertainty component pertaining to the second moment of inertia I is quantified through the quadrature summation method, treating dimensional measurement uncertainties as independent variables:

$$\Delta I = \sqrt{\left(\frac{\partial I}{\partial b}\Delta b\right)^2 + \left(\frac{\partial I}{\partial t}\Delta t\right)^2} \quad (2)$$

For a rectangular beam cross-section,

$$I = \frac{bt^3}{12} \quad (3)$$

the corresponding partial derivatives are:

$$\frac{\partial I}{\partial b} = \frac{t^3}{12}, \quad \frac{\partial I}{\partial t} = \frac{bt^2}{4} \quad (4)$$

Combining these expressions yields the propagated uncertainty in the second moment of area:

$$\Delta I = \sqrt{\left(\frac{t^3}{12}\Delta b\right)^2 + \left(\frac{bt^2}{4}\Delta t\right)^2} \quad (5)$$

C.2 Identification and Classification of Experimental Deviations

Notwithstanding stringent adherence to experimental protocol, numerous systematic and random contributors generate discrepancies between observed measurements and predicted theoretical values:

- **Support Condition Deviation:** Laboratory implementations approximate idealized simply supported, cantilever, and fully fixed configurations. Practical constraints such as fixture compliance, localized deformation at support points, and partial constraint effects diminish the effective rigidity compared to theoretical models.
- **Instrument Precision Limitations:** Dial gauges exhibit inherent measurement resolution constraints. Incomplete zeroing procedures and calibration drift introduce systematic biases into successive deflection measurements.
- **Distributed Load Effects:** Applied loads, whilst conceptually modeled as concentrated point actions, exhibit finite contact dimensions and potential off-center positioning relative to the theoretical load axis.

- **Material Property Variability:** The analytical model assumes homogeneous material characteristics with constant Young's modulus. Manufacturing tolerances, compositional heterogeneity, and residual stress distributions cause actual elastic properties to deviate from nominal specifications.
- **Geometric Nonlinearity Inception:** Classical beam theory presupposes infinitesimal displacements and linear elastic material response. Higher load magnitudes may introduce subtle geometric effects, particularly in slender cantilever configurations, that violate these foundational assumptions.
- **Environmental and Observational Perturbations:** Transient mechanical disturbances, thermal fluctuations in ambient conditions, and parallax/reading errors during dial indicator observation contribute additional measurement scatter.

C.3 Experimental Validity and Error Envelope

Whilst numerous uncertainty mechanisms operate concurrently, the experimental observations demonstrate close adherence to theoretical projections. Residual deviations fall within the acceptable tolerance band anticipated for tabletop-scale structural mechanics inves-

tigations, thereby affirming the applicability of classical Euler-Bernoulli formulations and reciprocal load-deflection relationships within the measured uncertainty bounds.

IX. FINAL OBSERVATIONS AND SUMMARY

The experimental investigation of cantilever and simply supported beam configurations successfully demonstrated the validity of foundational Euler-Bernoulli beam theory governing structural deformation. Proportional correspondence between applied loading and resulting deflection was consistently observed across all tested materials, with material stiffness effects clearly manifested—steel specimens exhibited minimal deflection whilst aluminium exhibited pronounced displacement under identical loading conditions. Comparative analysis of analytical predictions, numerical finite-element results, and laboratory measurements revealed substantial agreement, with minor divergences attributable to practical factors including boundary condition imperfections and material inhomogeneity. The integration of experimental validation, computational modeling, and theoretical analysis establishes a comprehensive framework for understanding and predicting structural behavior, thereby reinforcing the foundational principles of mechanics of materials and structural analysis for engineering applications.